ISTANBUL TECHNICAL UNIVERSITY ★ GRADUATE SCHOOL OF SCIENCE ENGINEERING AND TECHNOLOGY

CROSS-CUTTER SYSTEM LOAD TORQUE ANALYSIS, SYSTEM CONTROL AND SIMULATION

M.Sc. THESIS

Baturalp AKSOY

Department of Mechatronics Engineering

Mechatronics Engineering Programme

JUNE 2013

ISTANBUL TECHNICAL UNIVERSITY ★ GRADUATE SCHOOL OF SCIENCE ENGINEERING AND TECHNOLOGY

CROSS-CUTTER SYSTEM LOAD TORQUE ANALYSIS, SYSTEM CONTROL AND SIMULATION

M.Sc. THESIS

Baturalp AKSOY
(518101007)

Department of Mechatronics Engineering

Mechatronics Engineering Programme

Thesis Advisor: Asst. Prof. Ali Fuat ERGENÇ

JUNE 2013

İSTANBUL TEKNİK ÜNİVERSİTESİ ★ FEN BİLİMLERİ ENSTİTÜSÜ

DÖNEL BIÇAKLI KESME SİSTEMLERİNDE YÜK TORKU ANALİZİ, SİSTEM KONTROLÜ VE SİMÜLASYONU

YÜKSEK LİSANS TEZİ

Baturalp AKSOY
(518101007)

Mekatronik Mühendisliği Anabilim Dalı

Mekatronik Mühendisliği Programı

Tez Danışmanı: Yar. Doç. Ali Fuat ERGENÇ

HAZİRAN 2013

Baturalp Aksoy, a M.Sc. student of ITU Institute of Science student ID 518101007, successfully defended the thesis entitled **"**APPLICATION OF A MATRIX TECHNIQUE FOR DOMINANT POLE PLACEMENT OF DISCRETE-TIME TIME-DELAYED SYSTEMS ON A CROSS-CUTTER SYSTEM", which he prepared after fulfilling the requirements specified in the associated legislations, before the jury whose signatures are below.

Thesis Advisor :	**Asst. Prof. Ali Fuat ERGENÇ** Istanbul Technical University	....
Jury Members :	**Asst. Prof. Pınar BOYRAZ** Istanbul Technical University	....
	Asst. Prof. Özgür Turay KAYMAKÇI Yıldız Technical University	....

Date of Submission : 3 May 2013
Date of Defense : 11 June 2013

To my family,

FOREWORD

Cross-cutter systems are simple rotary systems that are widely used in the industry to cut sheet metal, paper and the like with a rotary knife motion. However these systems present a unique example which has two different movement zones and native time delay in their speed responses. This thesis takes on the control problem of this unique system with a different discrete time matrix approach for time delayed systems.

I would like to present my sincerely thanks to my advisor Asst. Prof. Ali Fuat ERGENÇ who has helped me in all layers of the problem and the solution.

May 2013 Baturalp AKSOY

TABLE OF CONTENTS

Page

ABBREVIATIONS

MSO	**:** Motion Servo On
MSF	**:** Motion Servo Off
MAJ	**:** Motion Axis Jog
TON	**:** Timer On Delay

LIST OF TABLES

Page

LIST OF FIGURES

Page

CROSS-CUTTER SYSTEM LOAD TORQUE ANALYSIS, SYSTEM CONTROL AND SIMULATION

SUMMARY

The cross-cutter system consists of a conveyor belt that is driven by a servo-motor, a rotary knife that is also driven by a servo-motor and two optical sensors which are directly positioned above the conveyor belt within a certain distance from the rotary knife.

The cross cutter system will be modeled along with the load torque that is driven by the cutting operation. This system will be controlled with a PID controller and simulations will be conducted to determine cutting efficiency.

The linear velocity of the rotary knife must be equal to the linear velocity of the conveyor belt within the range where the cutting operation occurs to avoid any strain and deformation on the material web. This constraint reveals two different movement zones for the rotary knife: The synchronization move and the make-up move.

The cut length will vary within three different cases depending on the knife velocity assuming the belt velocity is constant.

If the rotary knife has a constant velocity that is equal to the conveyor belt velocity in both its movement zones, consequently the cut length of the material will be equal to the circumference of the rotary knife body.

In the case where the cut length is chosen greater than the rotary knife circumference, the make up movement must be slower than the belt move to obtain greater length of material passing under the rotary knife in the same amount of time.

In the case where the cut length is chosen smaller than the rotary knife circumference, the make up movement must be faster than the belt move to obtain lesser length of material passing under the rotary knife in the same amount of time.

Test environment of this thesis is the cross cutter system which is located in Control Engineering Power and Motion Control Laboratory under the name of Rotary Knife Motion Control Experiment Set.

Both the rotary knife and the conveyor belt servo-motors are driven by Allen-Bradley Kinetix 6000 Servo Drives which are controlled by inputs from an Allen-Bradley Logix 5563 PLC. PLC routines are written using RSLogix 5000 Professional software. All components listed herein are products of Rockwell Automation.

A detailed analysis of acting forces during the cutting operation is conducted and A PID controller is designed to control the rotary knife velocity. The results are simulated and error rates are calculated for different piece lenght cases.

DÖNEL BIÇAKLI KESME SİSTEMLERİNDE YÜK TORKU ANALİZİ, SİSTEM KONTROLÜ VE SİMÜLASYONU

ÖZET

Çapraz kesici sistem, bir servo motor tarafından tahrik edilen bir konveyör, aynı zamanda, bir servo motor ve belli bir mesafede olan taşıyıcı kayış üzerinde konumlandırılmış iki optik sensör ve servomotor ile tahrik edilen bir dönel bıçaktan oluşmaktadır.

Kesici sistem ve kesme operasyonundan doğan yük torku bu tezde modellenecek ve bir PID kontrolör aracılığıyle kontrol edilecektir. Kontrol edilen sistemin simulasyonu yapılarak parça kesme işlemindeki hata oranları bulunacaktır.

Dönel bıçak doğrusal hız kesme işlemi malzeme tabakası üzerinde herhangi bir yük ve deformasyonunu önlemek için belirlenmiş senkronizasyon aralığında konveyör bandın doğrusal hızına eşit olması gerekir. Bu kısıtlama dönel bıçağı için iki farklı hareket bölgesi ortaya koymaktadır. Senkronizasyon hareket ve yetişme hareketi.

Kesme uzunluğu konveyor bandın hızı sabit kabul edilirse bıçak hızına bağlı olarak üç farklı durumda incelenir.

Dönel bıçak her iki hareket bölgesinde verilen konveyör bant hızına eşit sabit bir hızda ise, malzemenin kesme uzunluğu dönel bıçak gövdesinin çevresine eşit olacaktır.

Kesme uzunluğu dönel bıçak çevresinden daha büyük seçildiği durumda yetişme hareketinin, aynı zaman aralığında dönel bıçak altından geçen malzemenin daha uzun olması için kayış hareketinden daha yavaş olması gerekir.

Kesme uzunluğu dönel bıçak çevresinden daha küçük seçildiği durumda ise yetişme hareketinin, aynı zaman aralığında dönel bıçak altından geçen malzemenin daha kısa olması için kayış hareketinden daha hızlı olması gerekir.

İki fiber optik sensör malzeme uzunluğu geribildirimini sağlamak için dönel bıçaktan önce konumlandırılmıştır. Sensörlerden gelen farklı geri bildirimlere göre konveyör bant üzerindeki işaretler uzunlukları atamak için kodlanabilir.

Bu tezin test ortamı Dönel Bıçak Hareket Kontrol Deney Seti adı altında Kontrol Mühendisliği Güç ve Hareket Kontrol Laboratuvarında bulunan dönel bıçaklı kesici sistemidir.

Dönel bıçak ve konveyör bant servomotorları Allen-Bradley Kinetix 6000 Servo Sürücüler tarafından tahrik edilmektedir. Sürücü girişleri Allen-Bradley Logix 5563 PLC tarafından kontrol edilir. PLC rutinleri RSLogix 5000 Professional yazılımı kullanılarak yazılır. Burada listelenen tüm bileşenleri Rockwell Automation ürünüdür.

Kesme operasyonu sırasında oluşan güçlerin detaylı bir analizi yapılmıştır ve dönel bıçak hızını kontrol etmek için bir PID kontrolör tasarlanmıştır.

Sonuçlar simülasyona sokularak farklı parça boyları için kesme durumları incelenerek hata oranları hesaplanmıştır.

1. INTRODUCTION

1.1 Purpose of Thesis

This thesis will take on a cross-cutter system with a rotary knife and a conveyor belt to obtain a correct mathematical model of the comlete system motion and subsequently apply a matrix technique for dominant pole placement in this time-delayed system.

1.2 Introduction of the Cross-Cutter System

The cross-cutter system consists of a conveyor belt that is driven by a servomotor, a rotary knife that is also driven by a servomotor and two optical sensors, which are directly positioned above the conveyor belt within a certain distance from the rotary knife.

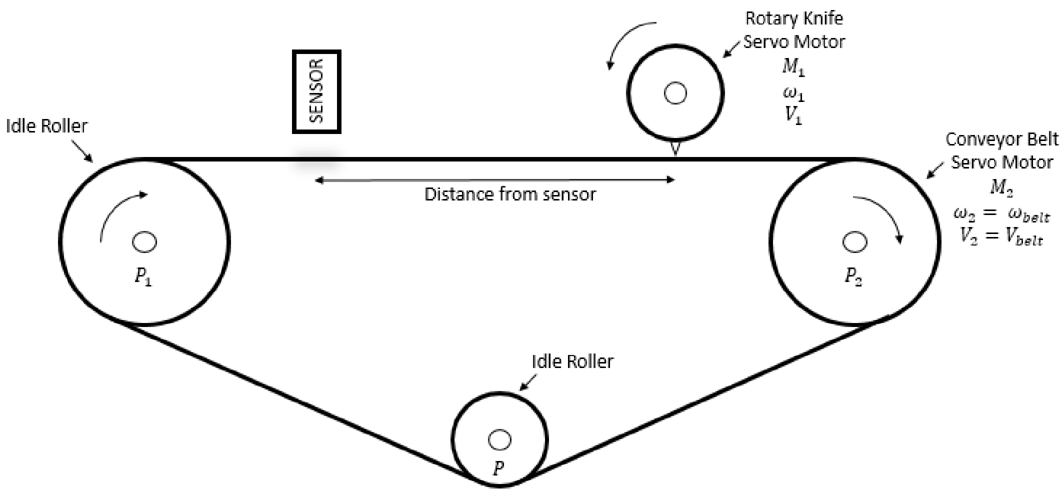

Figure 1.1 : Cross-cutter conveyor system. (View from side)

The conveyor belt has 3 axis points that are positioned triangularly with respect to each other. This is a common disposition which facilitates the removal of the belt when and if necessary. The rightmost pulley in Figure 1.1, depicted as P_2 is driven by a servo-motor which will allow velocity (ω_2) feedback and control. The other two pulleys which are depicted in Figure 1.1 as P_1 and P_2 are idle rollers without a motor in the setup this thesis will use.

A photo of the system is given in Figure 1.2.

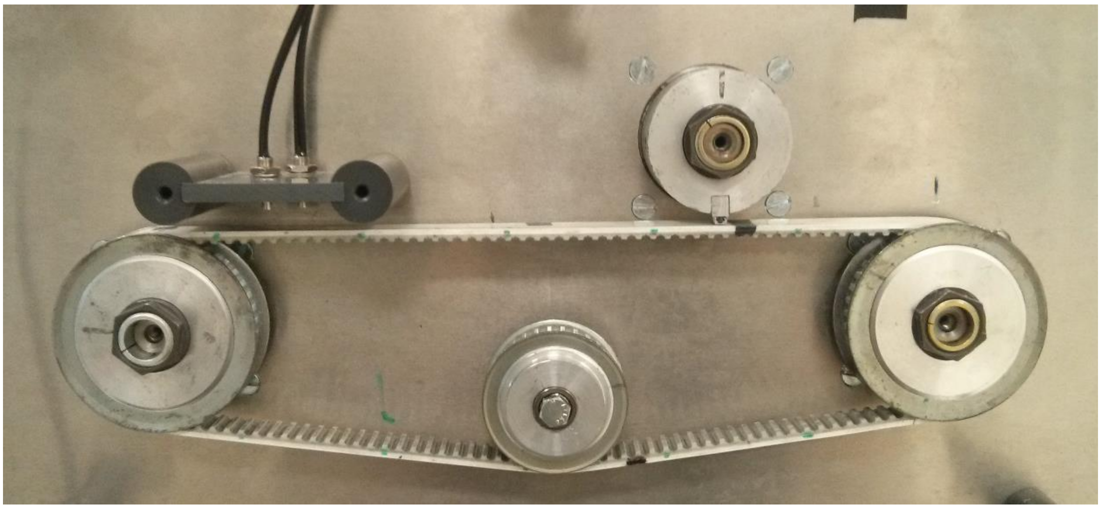

Figure 1.2 : Cross-cutter system

The rotary knife is driven by a servomotor and consists of a circular body and a triangular bulge on the outer diameter representing the cutter-knife. This body rotates around the servo-motor axis to symbolically cut the web of material carried by the conveyor belt as depicted in Figure 1.2.

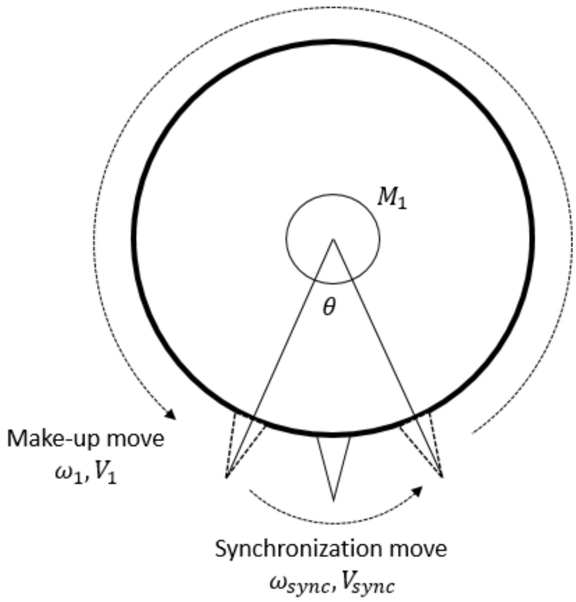

Figure 1.3 : Rotary knife movements

The linear velocity of the rotary knife V_{sync} must be equal to the linear velocity of the conveyor belt V_{belt} within the range θ shown in Figure 1.3 where the cutting operation occurs to avoid any strain and deformation on the material web. This constraint reveals two different movement zones for the rotary knife: The synchronization move and the make-up move.

The cut length l_{cut} will vary within 3 different cases depending on the knife velocity V_{knife} assuming the belt velocity V_{belt} is constant.

Case 1:

If the rotary knife has a constant velocity V_{knife} that is equal to the conveyor belt velocity V_{belt} in both its movement zones (make up move and synchronization move), consequently the cut length of the material l_{cut} will be equal to the circumference C_{knife} of the rotary knife body.

$$V_{makeup} = V_{sync} = V_{knife} = V_{belt} \xrightarrow{yields} l_{cut} = C_{knife} = 2\pi r_{knife} \tag{1.1}$$

Case 2:

In the case where the cut length l_{cut} is chosen greater than the rotary knife circumference C_{knife}, the make up movement must be slower than the belt move to obtain greater length of material passing under the rotary knife in the same amount of time t.

$$V_{makeup} < V_{belt} \xrightarrow{yields} l_{cut} > C_{knife} \tag{1.2}$$

Case 3:

In the case where the cut length l_{cut} is chosen smaller than the rotary knife circumference C_{knife}, the make up movement must be faster than the belt move to obtain lesser length of material passing under the rotary knife in the same amount of time t.

$$V_{makeup} > V_{belt} \xrightarrow{yields} l_{cut} < C_{knife} \tag{1.3}$$

Two fiber optical sensors are positioned before the rotary knife to allow material length feedback based on markings on the material web as seen in Figure 1.4. The feedback from the sensors could be encoded to assign lenghts to different feedbacks.

To give an arbitrary example: Single marker on the right could mean $50mm$ whereas double markers could mean $75mm$ and single marker on the left could mean $25mm$.

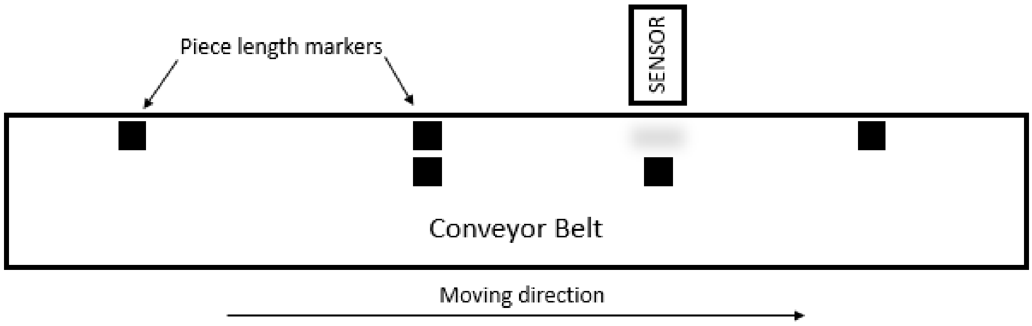

Figure 1.4 : Piece length sensor function. (View from top).

A photo of the sensors is given in Figure 1.5.

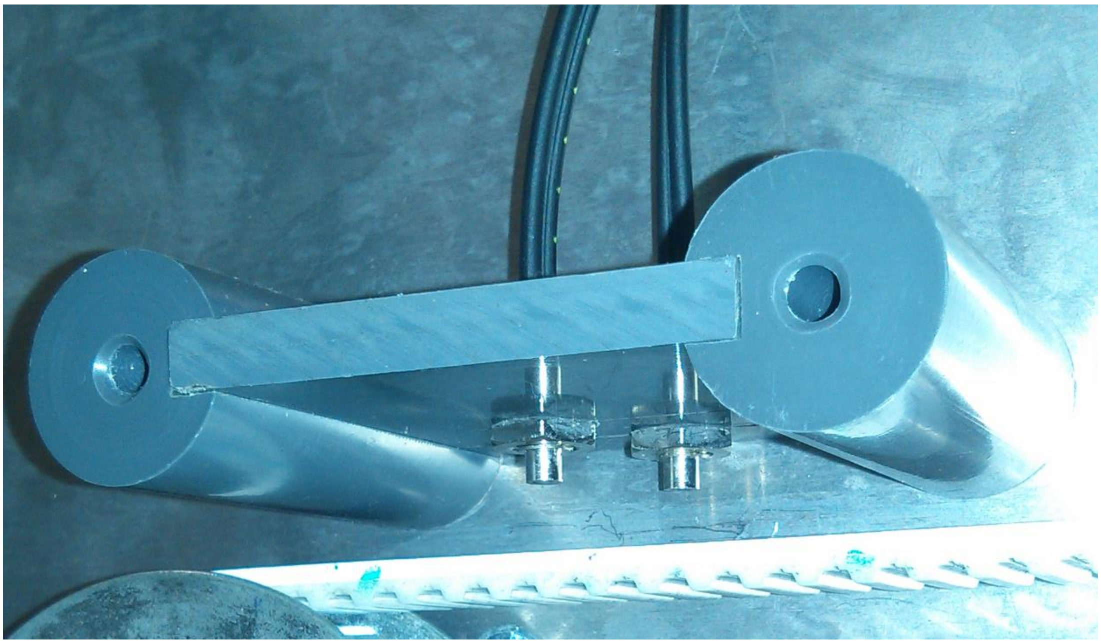

Figure 1.5 : Piece length sensors

1.3 System Configuration

Test environment of this thesis is the cross-cutter system, which is located in Control Engineering Power and Motion Control Laboratory under the name of Rotary Knife Motion Control Experiment Set.

Both the rotary knife and the conveyor belt servo-motors are driven by Allen-Bradley Kinetix 6000 Servo Drives as seen in Figure 1.6.

Figure 1.6 : Allen Bradley Kinetix 6000

These drives are controlled by inputs from an Allen-Bradley Logix 5563 PLC which is shown in Figure 1.7.

Figure 1.7 : Allen Bradley Logix 5563 PLC

PLC routines are written using RSLogix 5000 Professional software. All components listed herein are products of Rockwell Automation.

2. SYSTEM ANALYSIS

2.1 PLC Routine

A simple main routine is written within RSLogix 5000 as seen in Figure 2.1 using ladder programming to give speed inputs to the rotary knife servo-motor and to obtain a closed loop system response for this input. Programming blocks used in the routine are motion blocks, timer blocks and positive/negative switch blocks as seen in Table 2.1.

Table 2.1 : RSLogix 5000 Motion Blocks Used In Rotary Knife Modelling Routine

Code	Name	Description
MSO	Motion Servo On	Activates the drive amplifier and servo loop for the axis.
MSF	Motion Servo Off	Deactivates the drive output and servo loop for the axis.
MAJ	Motion Axis Jog	Moves an axis at a constant speed until stop input received.
TON	Timer On Delay	Non-retentive timer that accumulates time when enabled.

Rotary knife servo-motor is defined within the motion group as AXIS_02_Knife. Two boolean variables named “ServoOn” and “start” are defined to act as software switches in the routine. Two other variables “timer” and “timer2” are defined to be used in timer (TON) motion blocks. Lines of the ladder routine are referred as “rungs”.

A velocity trend is defined to track both “AXIS_02_Knife.ActualVelocity” and “AXIS_02_Knife.CommandVelocity” signals to obtain a graph representation of the input and output velocity values. This trend is triggered by the routine in Figure 2.1. The movement of the rotary knife is sampled using $1ms$ sample size in this trend.

Rotary knife axis is controlled by a velocity gain PI controller within the PLC. An arbitrary proportional gain $K_{p_{knife}} = 255,14368$ and an arbitrary integral gain $K_{I_{knife}} = 20,0$ are set within the PI controller for the AXIS_02_Knife.

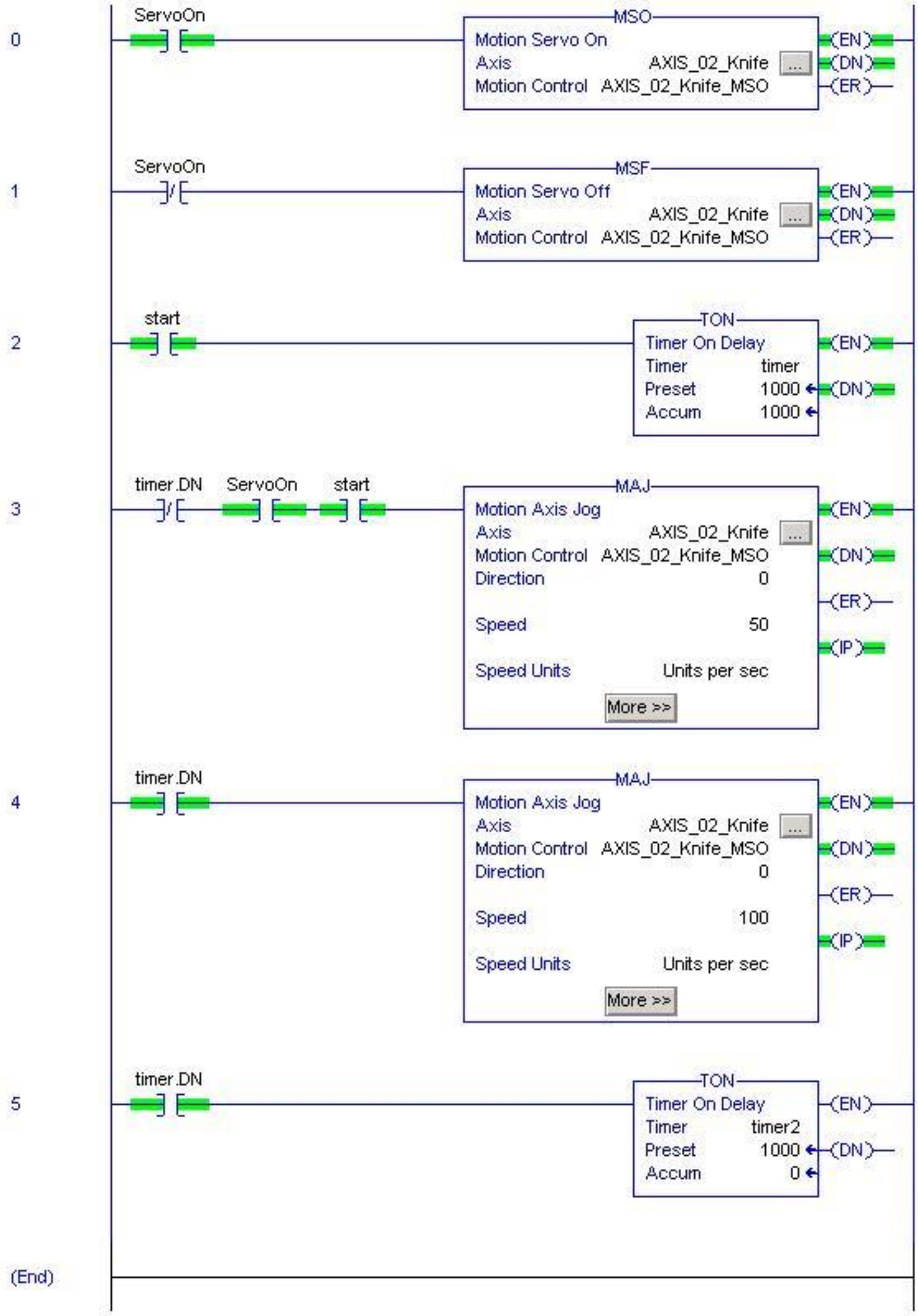

Figure 2.1 : Rotary knife modelling routine

The routine in Figure 2.1 is explained step by step as follows:

When the soft switch “ServoOn” is closed, the drive amplifier and the servo loop for the rotary knife servo-motor axis (AXIS02_Knife) is activated by the MSO motion block.

When the soft switch “ServoOn” is open, the MSF block is active. This means the servo loop is deactivated.

When the “start” switch is also closed alongside with “ServoOn” switch, the first timer which counts towards $1000ms$ is enabled. At the same time, MAJ motion block on rung 3 is activated. This block moves the depicted AXIS02_Knife at a constant speed given as $50\ units$ within the block.

In rung 3 MAJ motion block has a switch before it with the variable “timer.DN” which is the DN bit of the first TON block that is used. This switch ensures that when the timer has accumulated the given $1000ms$ and the DN bit is enabled, the MAJ motion block on rung 3 is deactivated.

The same bit “timer.DN” switches the MAJ motion block on rung 4 enabling it. When enabled MAJ motion block on rung 4 moves the depicted AXIS02_Knife at a constant speed given as $100\ units$ within the block.

The same bit “timer.DN” switches the second timer block TON on rung 5 which also counts towards 1000ms after which it enables the “timer2.DN” bit.

The “start” bit is used to trigger the start of the velocity trend and the “timer2.DN” bit is used to trigger the stop of velocity trend.

As a result of the routine the trend in Figure 2.2 is obtained and exported to MATLAB environment for calculations.

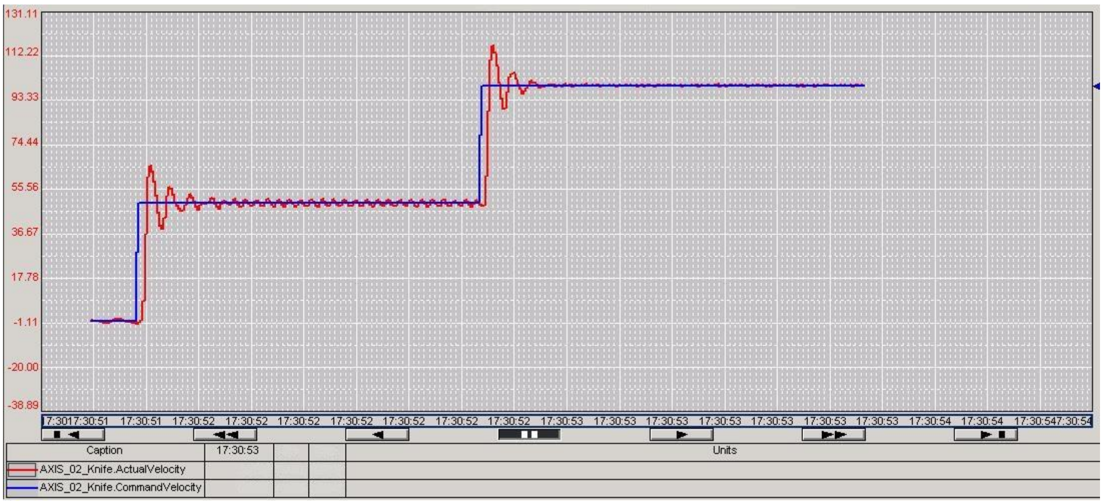

Figure 2.2 : Rotary knife velocity trend screenshot.

Exported values are plotted in MATLAB using the m file depicted in Figure 2.3.

```
clear all
clc

A = xlsread('b.xlsx') ;
plot(0.001*A(:,1),A(:,2),0.001*A(:,1),A(:,3))
grid on
```

Figure 2.3 : Importing and plotting knife velocity trend data into MATLAB.

2.2 Obtaining Rotary Knife Mathematical Model

Plotted rotary knife velocity response shows actual velocity against the input velocity in Figure 2.4. This plot and the imported data will be used to obtain a mathematical model for the rotary knife servo-motor and drive.

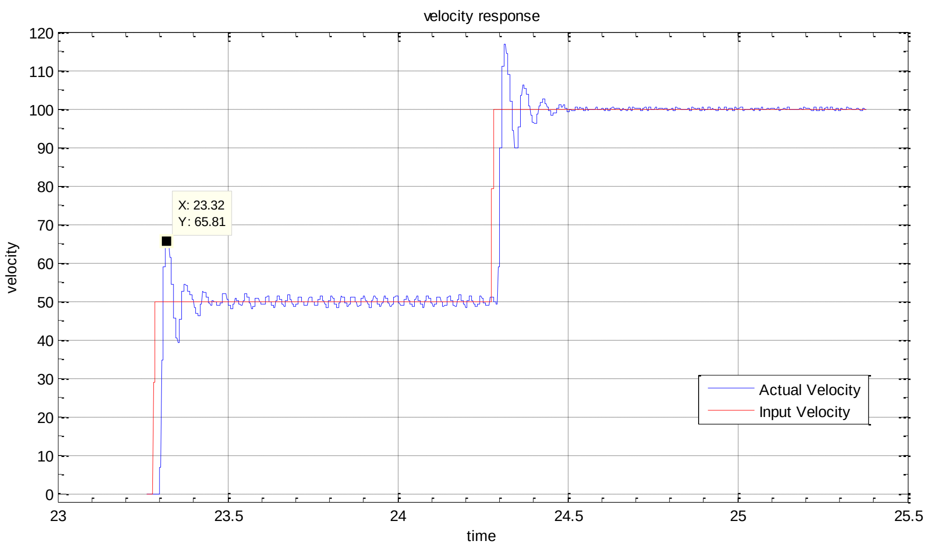

Figure 2.4 : Rotary knife velocity step input response.

Overshoot $M_{p_{knife}}$ and peak time $T_{p_{knife}}$ is obtained from the imported data as following:

$$M_{p_{knife}} = \frac{\omega_{max} - \omega_{ref}}{\omega_{ref}} = \frac{131,573 - 100}{100} = 31,57\% \qquad \textbf{(2.1)}$$

$$T_{p_{knife}} = t_{peak} - t_{input} 19{,}037 - 19{,}011 = 0{,}026\ s \tag{2.2}$$

$$\zeta = -\frac{\ln\left(M_{p_{knife}}\right)}{\sqrt{\left(\pi^2 + \ln\left(M_{p_{knife}}\right)^2\right)}} = 0{,}3445 \tag{2.3}$$

$$\omega_n = \frac{\pi}{T_{p_{knife}}\sqrt{1-\zeta^2}} = 128{,}7094 \tag{2.4}$$

The system response also has a $0.018s$ time delay.

Applying these values into the standard form of a second order system:

$$G_{mk}(s) = \frac{\omega_n^2}{s^2 + 2\zeta\omega_n s + \omega_n^2} = \frac{16566{,}1}{s^2 + 88{,}6813s + 16566{,}1} \tag{2.5}$$

This second order system is compared to the actual measured data and to the output of MATLAB system identification tool using the simulink model in Figure 2.5.

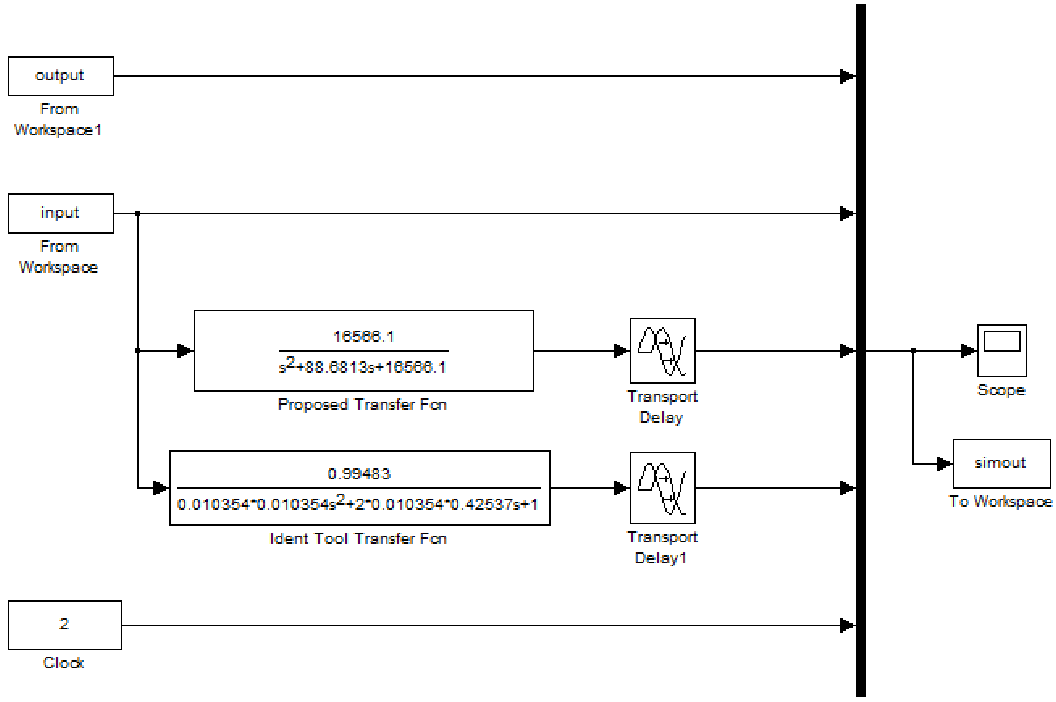

Figure 2.5 : Simulink model for system response comparison

The result plot of this simulink model is shown in Figure 2.6.

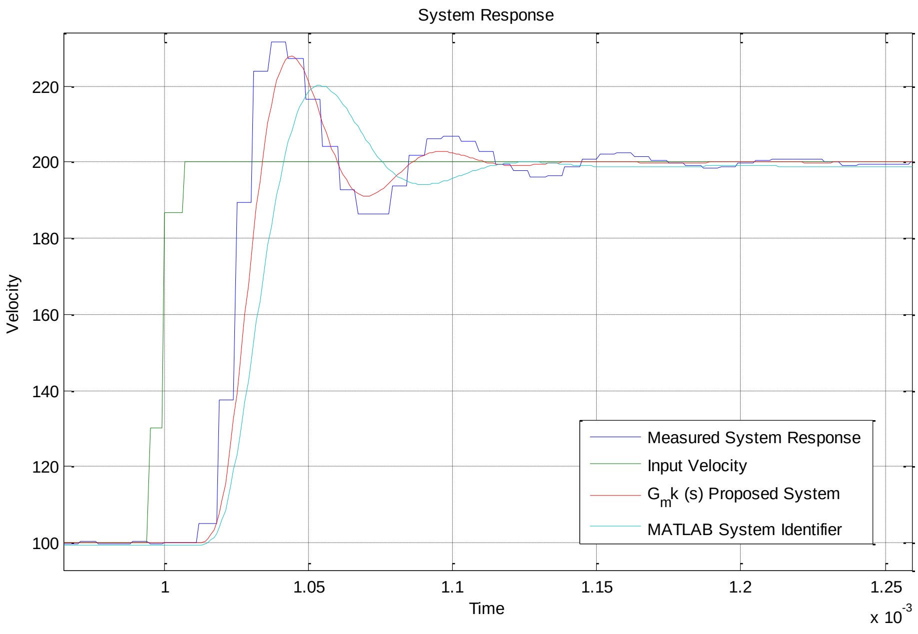

Figure 2.6 : System response comparison

Observed and plotted response belongs to the system of rotary knife servo-motor drive and PI controller. This system could be expressed using the block diagram in Figure 2.7.

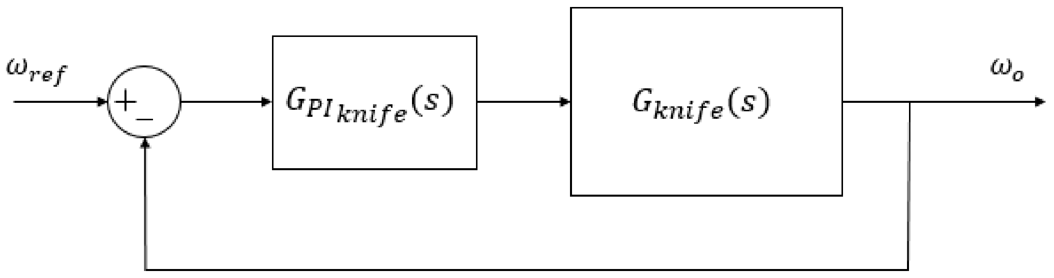

Figure 2.7 : Block diagram of rotary knife and controller

The system response obtained from the rotary knife velocity trend will be called $G_{mk}(s)$ as depicted in Figure 2.8.

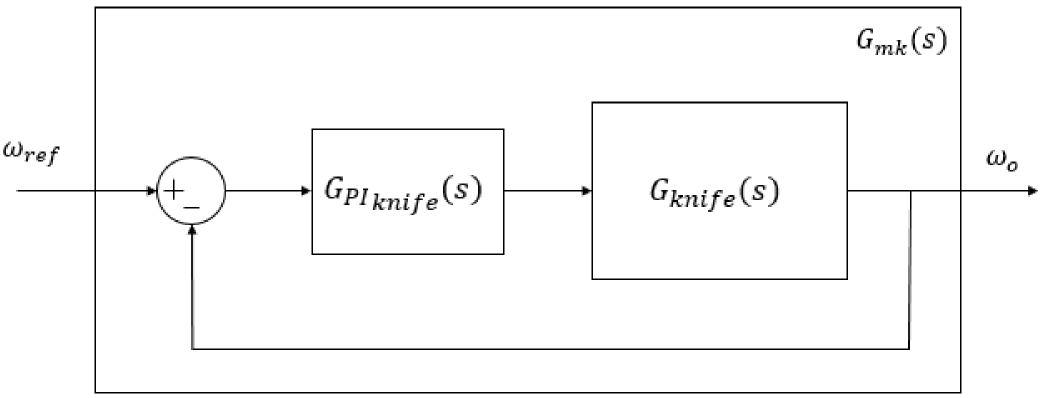

Figure 2.8 : Block diagram of rotary knife and controller

The transfer function for the rotary knife system $G_{knife}(s)$ will be derived from the obtained system response $G_{mk}(s)$ using the controller values proportional gain $K_{p_{knife}}$ and integral gain $K_{I_{knife}}$ from the PI controller $G_{PI_{Knife}}$.

$$G_{PI_{knife}}(s) = \frac{K_{p_{knife}} s + K_{I_{knife}}}{s} \tag{2.6}$$

From the block diagram in Figure 2.8:

$$G_{mk}(s) = \frac{G_{PI_{knife}}(s) G_{knife}(s)}{1 + G_{PI_{knife}}(s) G_{knife}(s)} \tag{2.7}$$

From here we derive G_{knife} as following:

$$G_{knife} = \frac{G_{mk}(s)}{G_{PI_{knife}}(s)\left(1 - G_{mk}(s)\right)} \tag{2.8}$$

As arbitrary values, proportional gain $K_{p_{knife}} = 255{,}14368$ and integral gain $K_{I_{knife}} = 20{,}0$ are set within the PI controller.

Using these values;

$$G_{PI_{knife}}(s) = \frac{K_{p_{knife}} s + K_{I_{knife}}}{s} = \frac{255{,}14368\, s + 20}{s} \tag{2.9}$$

Using Equation (2.5) and Equation (2.9) the transfer function of the rotary knife is obtained as following:

$$G_{knife} = \frac{64,9285}{s^2 + 88,7597s + 6,95148} \quad \textbf{(2.10)}$$

Obtained transfer function represents a second order system with two following open loop poles:

$$s_1 = -88,6813$$
$$s_2 = -0,783872 \quad \textbf{(2.11)}$$

2.3 Open Loop Root Locus

Open loop root-locus is represented in Figure 2.9. As one of the poles is more than 100 times far left in the root-locus, its effect rapidly decays and neglectible. Therefore, the system will behave similar to a first order system. The first root seen in Equation 2.11 represents the electrical section of the system while the second root s_2, mechanical section.

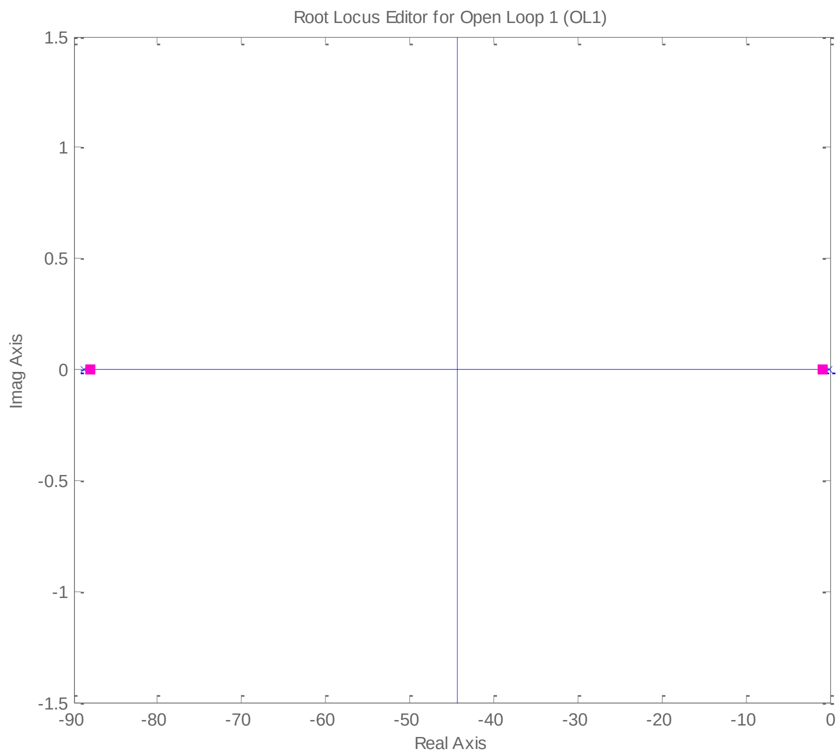

Figure 2.9 : Open loop root-locus of G_{knife}

3. CUTTING OPERATION

3.1 Enacting Forces in Cutting Operation

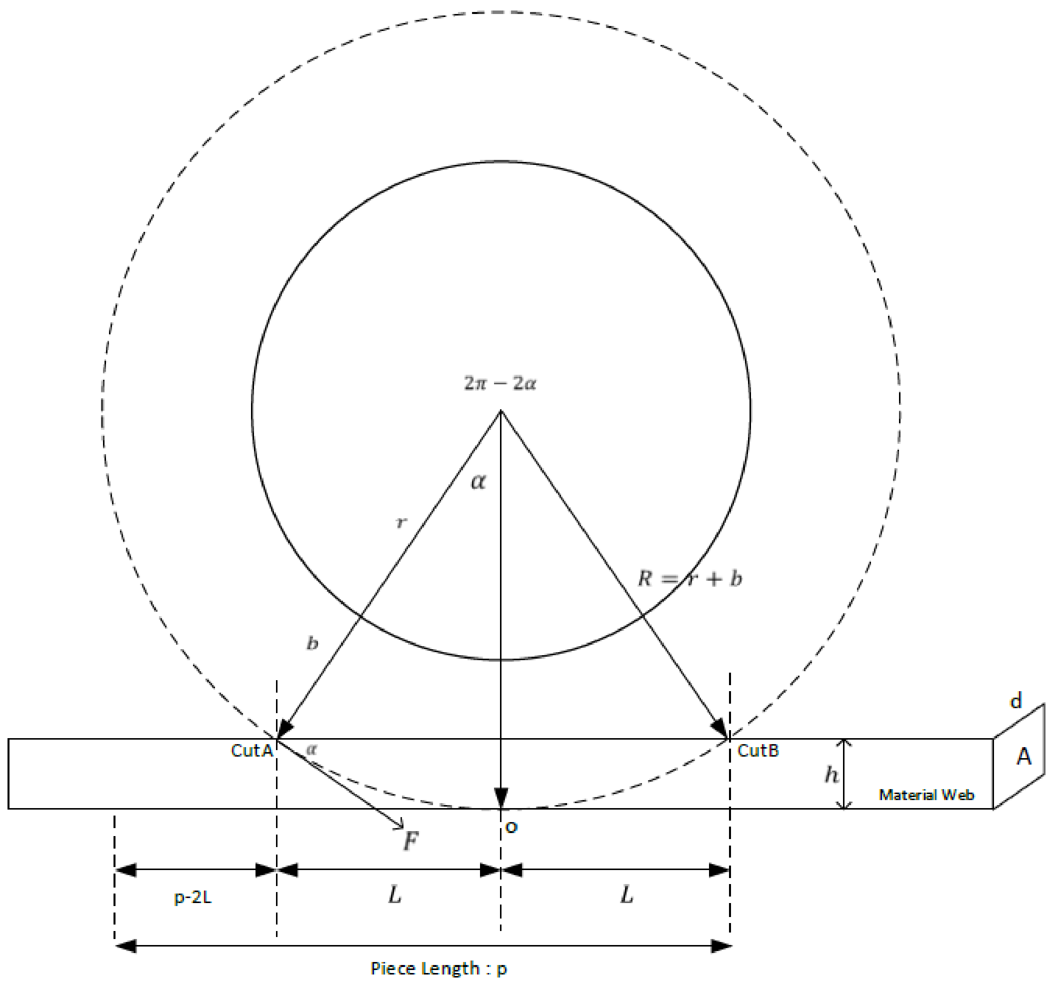

Figure 3.1: Rotary knife operative variables

To be able to understand the forces acting upon the rotary knife and the material web that is being cut, Figure 3.1 has been drawn.

In Figure 3.1, the inner circle represents the rotary knife body and the outer circle is the blade tip movement circumference.

Three arrows pointing towards the material web represent the cutting blade and its various positions upon the material web. These three positions are pointing to three point of interests for the movement.

The first one on the left is the first point that the blade tip touches the material web and the acting cutting force F is met with a resistance. This point is detoned as $cutA$ for future use in calculations.

The second position of the blade is the origin position o and the third one $cutB$ is the point where the blade leaves the material web.

The radius of the blade tip movement circumference, is denoted as R and the angle between the first cut position and the origin position of the blade is denoted as α.

$$\alpha = cos^{-1}\left(\frac{R-h}{R}\right) \qquad \textbf{(3.1)}$$

$sin\alpha$ is calculated below to be used in Equation 3.10.

$$sin\alpha = \frac{L}{R} \qquad \textbf{(3.1)}$$

$$L^2 + (R-h)^2 = R^2 \qquad \textbf{(3.2)}$$

$$L^2 = 2Rh - h^2 \qquad \textbf{(3.3)}$$

$$L = \sqrt{h(2R-h)} \qquad \textbf{(3.4)}$$

$$sin\alpha = \frac{\sqrt{h(2R-h)}}{R} \qquad \textbf{(3.5)}$$

Inside the cutting zone, the linear velocity of the rotary knife must be equal to the linear velocity of the material web to avoid any deformation to the material web.

$$V_{knife} = V_{belt} \qquad \textbf{(3.6)}$$

The cut begins at the point $cutA$ and continues until the blade reaches the origin point o. As the material web moves together with the blade tip during the cutting operation, the cut movement is stritctly vertical.

The movement of the blade tip, enacts as shear stress τ_{max} over the cross section of the material which is denoted as $A = h * d$. The thickness of the material is denoted as h and the width of the material web is denoted as d.

The shear stress τ_{max} causes a failure in the material when it is equal or greater than the ultimate tensile stress of the material σ_{uts}.

The material is chosen to allow a brittle failure and an ideal cut.

The reactive force from the material web creates a load torque T_L that enacts as an input into the rotary system from the time the cut begins at $cutA$ to the time blade reaches the origin point o.

$$T_L = \frac{F}{R} \tag{3.7}$$

$$T_m = \omega_m (J_m s + B_m) + T_L \tag{3.8}$$

$$\tau_{max} = \sigma_{uts} \tag{3.9}$$

T_L is calculated dependent to the ultimate tensile strength σ_{uts} , the blade tip movement radius R and the cross section of the material being cut $A = h * d$.

$$\tau_{max} = \frac{F sin\alpha}{A} = \frac{T_L sin\alpha}{R.h.d} = \frac{T_L\sqrt{\frac{2R}{h} - 1}}{R^2.d} = \sigma_{uts} \tag{3.10}$$

$$T_L = \sigma_{uts}.\frac{R^2 d}{\sqrt{\frac{2R}{h} - 1}} \tag{3.11}$$

3.2 Rotary Knife Velocity Analysis

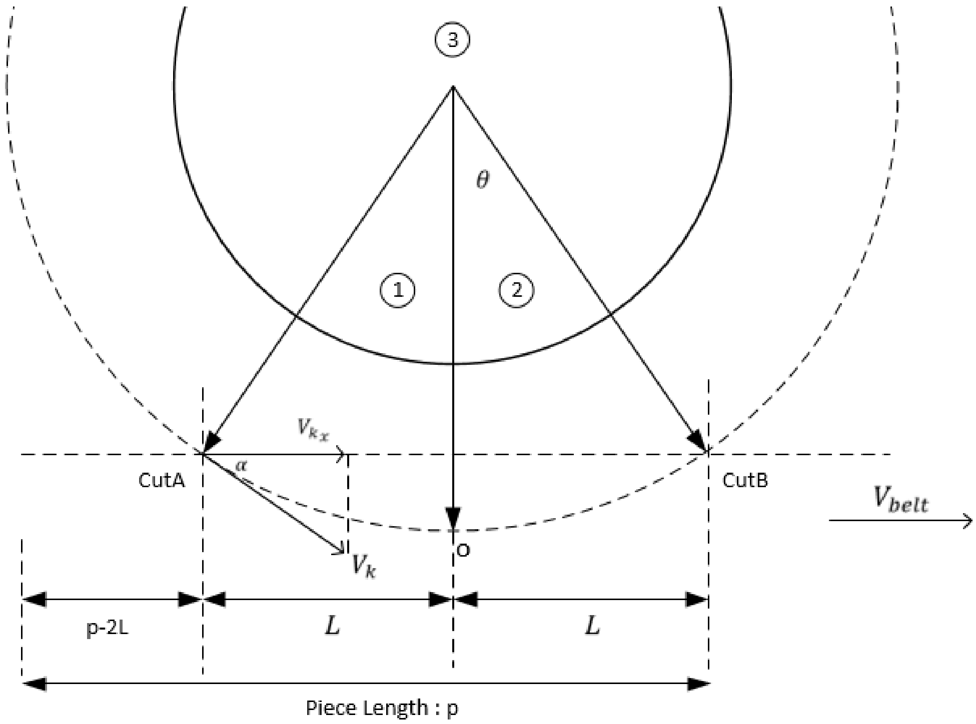

Figure 3.2: Rotary knife velocity and affecting variables

The cutting movement has 3 different zones: the first two zones: Zone 1 and Zone 2, are inside the actual cutting zone, the third one: Zone 3, is the catch-up zone.

3.2.1 Inside the cutting zone : Zones 1 and 2

Linear speed at the tip of the blade is denoted as:

$$V_k = \omega_k . R \quad \textbf{(3.12)}$$

The horizontal component of the blade tip speed is calculated in zones 1 and 2 in different ways.

In zone 2, the actual position angle θ is used to denote the speed equation.

$$V_{k_{x_2}} = V_k . cos\theta \quad \textbf{(3.13)}$$

In zone 1, the angle between the origin point o and the blade position can be denoted as $2\pi - \theta$. Therefore, the blade tip speed is calculated as:

$$V_{k_{x_1}} = V_k . \cos(2\pi - \theta) \qquad \textbf{(3.14)}$$

At this point, two equations become equal as a result of cosine function's trigonometric property:

$$\cos(2\pi - \theta) = \cos(\theta) \qquad \textbf{(3.15)}$$

As a result, in both zones 1 and 2 the blade tip speed's horizontal component is equal to:

$$V_{k_x} = V_k . cos\theta \qquad \textbf{(3.16)}$$

Inside the cutting zone, the the horizontal component of the blade tip speed V_{k_x} must be equal to the material web speed V_{belt}.

$$V_{belt} = V_{k_x} = V_k . cos\theta \qquad \textbf{(3.17)}$$

$$V_k = \frac{V_{belt}}{cos\theta} \qquad \textbf{(3.18)}$$

3.2.2 Inside the catch-up zone: Zone 3

Inside the catch-up zone, angular distance to be covered is $2\pi - 2\alpha$, therefore the catch-up time t_{cu} is calculated as seen in Equation 3.19.

$$t_{cu} = \frac{2\pi - 2\alpha}{\omega_k} \qquad \textbf{(3.19)}$$

In this zone, the piece lenght will determine the rotary knife speed as the aim is to catch-up just in time to cut the end of the piece.

Therefore the catch-up time t_{cu} is also the duration in which the conveyor belt covers the distance between the end of the piece and the point $cutA$. This distance could be denoted as $p - 2L$.

$$t_{cu} = \frac{p - 2L}{V_{belt}} \qquad \textbf{(3.20)}$$

Using Equation 3.19 and Equation 3.20,

$$t_{cu} = \frac{2\pi - 2\alpha}{\omega_k} = \frac{p - 2L}{V_{belt}} \quad \textbf{(3.21)}$$

Where $\omega_k = \frac{V_k}{R}$,

$$\frac{R(2\pi - 2\alpha)}{V_k} = \frac{p - 2L}{V_{belt}} \quad \textbf{(3.22)}$$

$$V_k = V_{belt}\frac{R(2\pi - 2\alpha)}{p - 2L} \quad \textbf{(3.23)}$$

$$V_k = V_{belt}\frac{R(2\pi - 2\cos^{-1}\left(\frac{R-h}{R}\right))}{p - 2\sqrt{h(2R-h)}} \quad \textbf{(3.24)}$$

3.3 Load Torque Input Argument

Input load torque is calculated in relation to material thickness and blade travel inside the material.

The blade travel is calculated in Equation 3.25:

$$BT = \frac{h - R(1 - cos\theta)}{h} \quad \textbf{(3.25)}$$

This thesis will assume that the load torque will be proportional to blade travel inside the material. Therefore,

$$T = T_L.BT \quad \textbf{(3.26)}$$

$$T = T_L.\frac{h - R(1 - cos\theta)}{h} \quad \textbf{(3.27)}$$

Input load torque should be saturated between cutA and 2pi as these are the limits to the cut zone.

Fourier series approach is used to saturate the load torque value:

$$T(\theta) = A_0 + \sum_{n=1}^{\infty} A_n \cos\left(\frac{n\pi\theta}{2\pi}\right) + \sum_{n=1}^{\infty} B_n \cos\left(\frac{n\pi\theta}{2\pi}\right) \quad \textbf{(3.28)}$$

Where coefficients are,

$$A_0 = \frac{1}{4\pi}\int_{cutA}^{2\pi} T(\theta)\, d\theta \quad \textbf{(3.29)}$$

$$A_0 = \frac{1}{4\pi}\int_{cutA}^{2\pi} T_L.\,(\,h - R(1 - cos\theta)\,)\, d\theta \quad \textbf{(3.30)}$$

$$A_n = \frac{1}{2\pi}\int_{cutA}^{2\pi} T(\theta) cos\left(\frac{n\pi\theta}{2\pi}\right)\, d\theta \quad \textbf{(3.31)}$$

$$A_n = \frac{1}{2\pi}\int_{cutA}^{2\pi} T_L.\,(\,h - R(1 - cos\theta)\,) cos\left(\frac{n\theta}{2}\right)\, d\theta \quad \textbf{(3.32)}$$

$$B_n = \frac{1}{2\pi}\int_{cutA}^{2\pi} T(\theta) sin\left(\frac{n\pi\theta}{2\pi}\right)\, d\theta \quad \textbf{(3.33)}$$

$$B_n = \frac{1}{2\pi}\int_{cutA}^{2\pi} T_L.\,(\,h - R(1 - cos\theta)\,) sin\left(\frac{n\theta}{2}\right)\, d\theta \quad \textbf{(3.34)}$$

The fourier series solution, while useful to saturate between required points, is very slow and cumbersome. Therefore another method for saturation is used:

$$T_{sat} = \frac{\sqrt{T^2} + T}{2} \quad \textbf{(3.35)}$$

3.4 Integration Into System Model

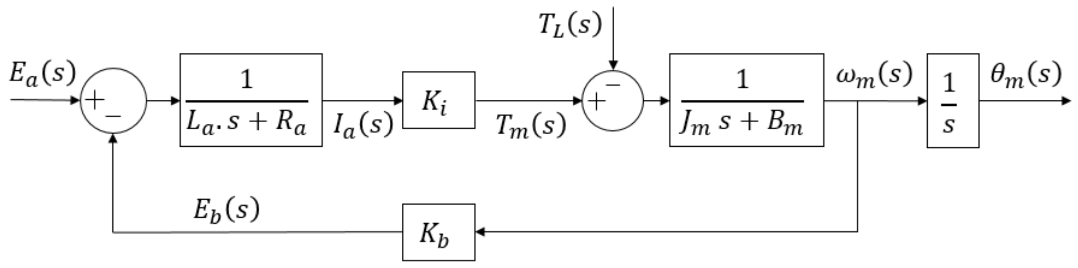

Figure 3.3: Rotary knife electric DC motor mathematical model

In Figure 3.3 depicted is a mathematical model of an electrical DC motor. To inlcude the obtained load torque T_L resulting from the cutting operation into the simulink model, the inertia and friction block must be considered. As seen in Figure 3.3, load torque input is affecting the system before the inertia and friction block.

The inertia and friction block must be seperated from the obtained system G_{knife} seen in Equation 2.10, to form a simulink model where the load torque T_L and its effect on the system could be observed.

To seperate the inertia and friction block, the following method is applied:

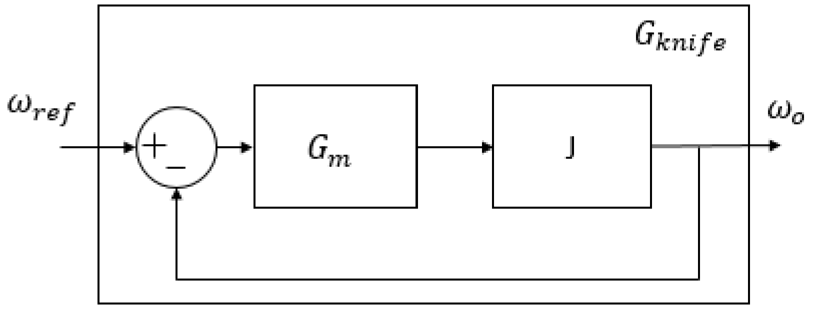

Figure 3.4: Rotary knife system inertia and friction block

As seen in Figure 3.4,

$$G_{knife} = \frac{G_m\, J}{1 + G_m\, J} \tag{3.36}$$

$$J = \frac{1}{J_m s + B_m} \tag{3.37}$$

Transfer function of the rotary knife motor without the inertia and friction coefficient are obtained as seen in Equation 3.38

$$G_m = \frac{G_{knife}}{J(1 - G_{knife})} \tag{3.38}$$

Motor inertia J_m and friction coefficient B_m are given as follows:

$$J_m = 0.000026\ kg.m^2$$
$$B_m = 0.001 \tag{3.39}$$

Using Equation 2.10 and Equation 3.38, Model of the motor G_m is obtained as seen in Equation 3.40.

$$G_m = \frac{G_{knife}}{J(1 - G_{knife})} = \frac{0.00168814s + 0.0649285}{s^2 + 88.7597s - 57.977} \tag{3.40}$$

Using the transfer function G_m and the mathematical model of the DC electric motor, a MATLAB Simulink model of the rotary knife system is obtained as seen in Figure 3.5.

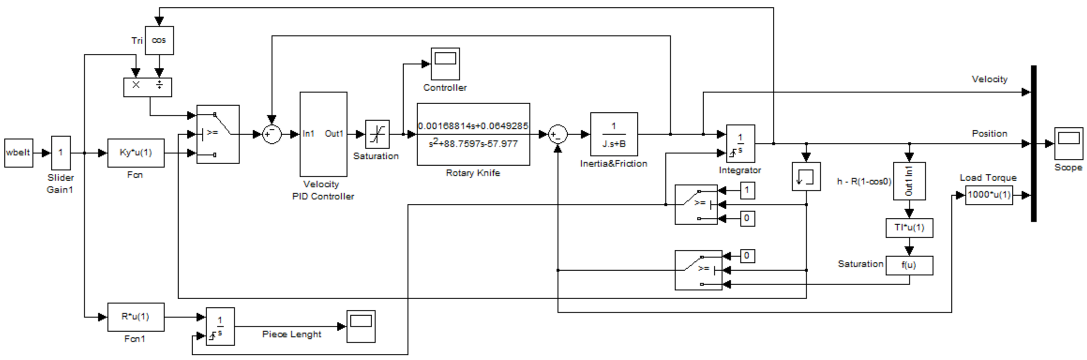

Figure 3.5: Rotary knife system Simulink model

A bigger representation of Figure 3.5 is available as Appendix B.

In the depicted model for simulation, the reference is given differently in two different working zones, the cutting zone and the catch-up zone.

Inside the catch-up zone, the reference is given as in Equation 3.18: $V_k = \frac{V_{belt}}{cos\theta}$ and inside the cutting zone;

The reference is given as in Equation 3.24: $V_k = V_{belt}\frac{R(2\pi-2\cos^{-1}\left(\frac{R-h}{R}\right))}{p-2\sqrt{h(2R-h)}}$

The reference input is given into the PID controller, which is designed according to empirical optimal settling time in Mathematica as seen in Appendix E.

The control signal is admitted into the system transfer function and load torque input is received just before the inertia and friction block. The output is integrated to calculate the position value as θ.

The load torque input is calculated using the Equation 3.11, and saturated using Equation 3.35. This input is being effective starting from point $cutA$ to the origin point as seen in Figure 3.2.

Actual cutted piece length is also calclulated within the simulation by integrating the conveyor belt speed, thus multiplying simulation time with the speed to obtain the piece length.

Three different cases are simulated with the denoted model.

3.4.1 Case1: Piece length is equal to rotary knife circumference

$$p = 2\pi R$$

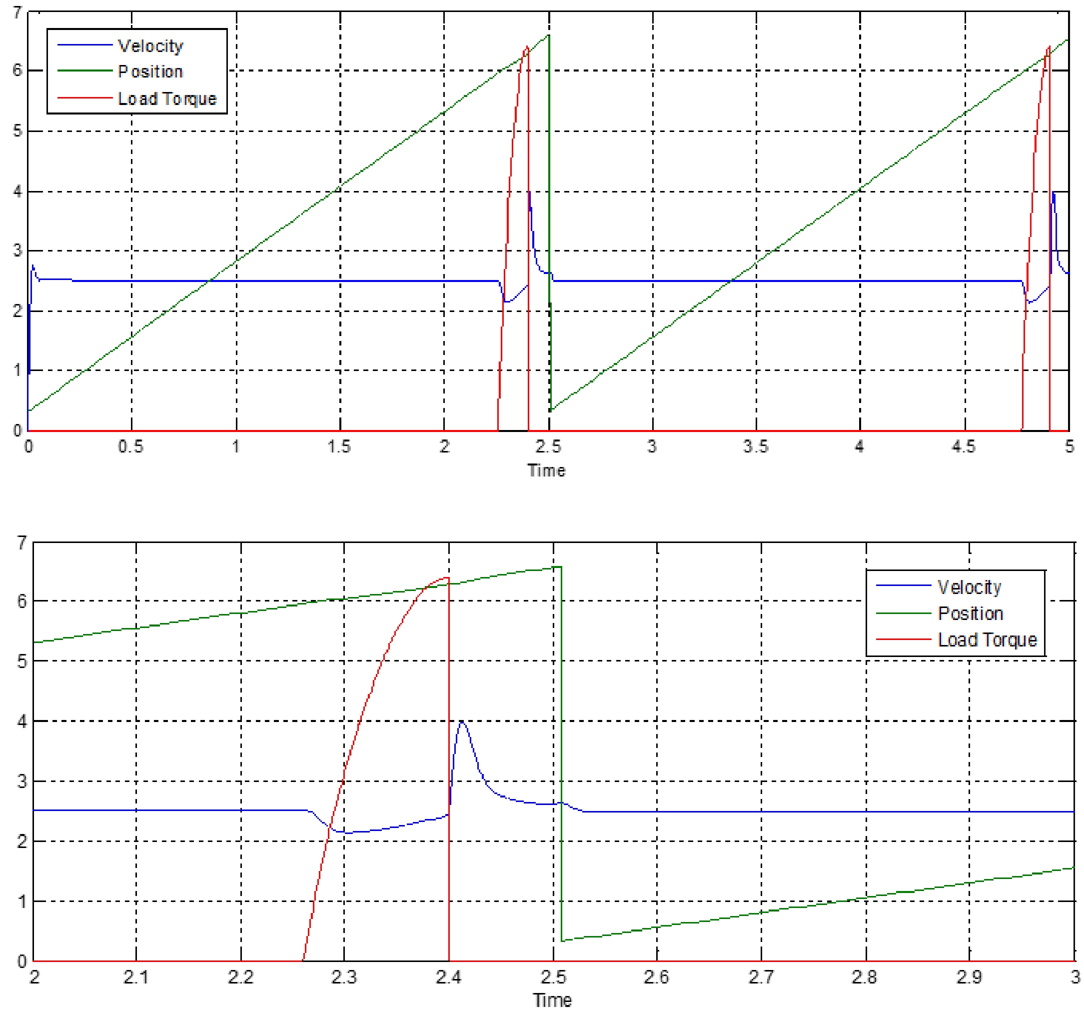

Figure 3.6: Piece length is equal to rotary knife circumference

As the piece length is equal to the rotary knife circumference, the speed in the catch-up zone and cutting zone are equal. The effect of the load torque (in red) could be observed in Figure 3.6.

The simulated actual cut piece length has an error of 0.23% in this case.

3.4.2 Case2: Piece length is bigger than the rotary knife circumference.

$$p > 2\pi R$$

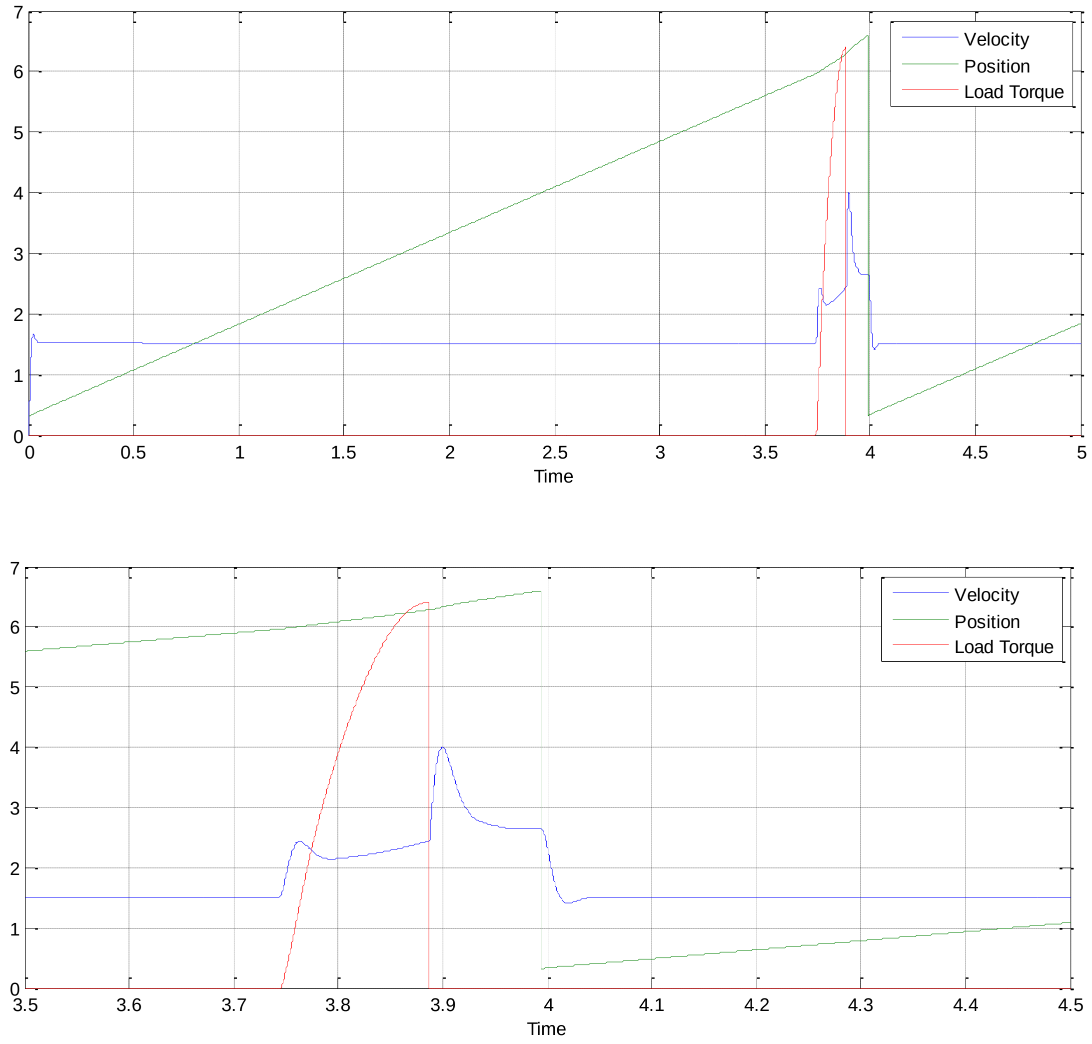

Figure 3.7: Piece length is bigger than the rotary knife circumference

As the piece length is bigger than the rotary knife circumference, the speed in the catch-up zone is slower than the speed in cutting zone. The effect of the load torque (in red) could be observed in Figure 3.7.

The simulated actual cut piece length has an error of 0.14% in this case.

3.4.3 Case3: Piece length is smaller than the rotary knife circumference

$$p < 2\pi R$$

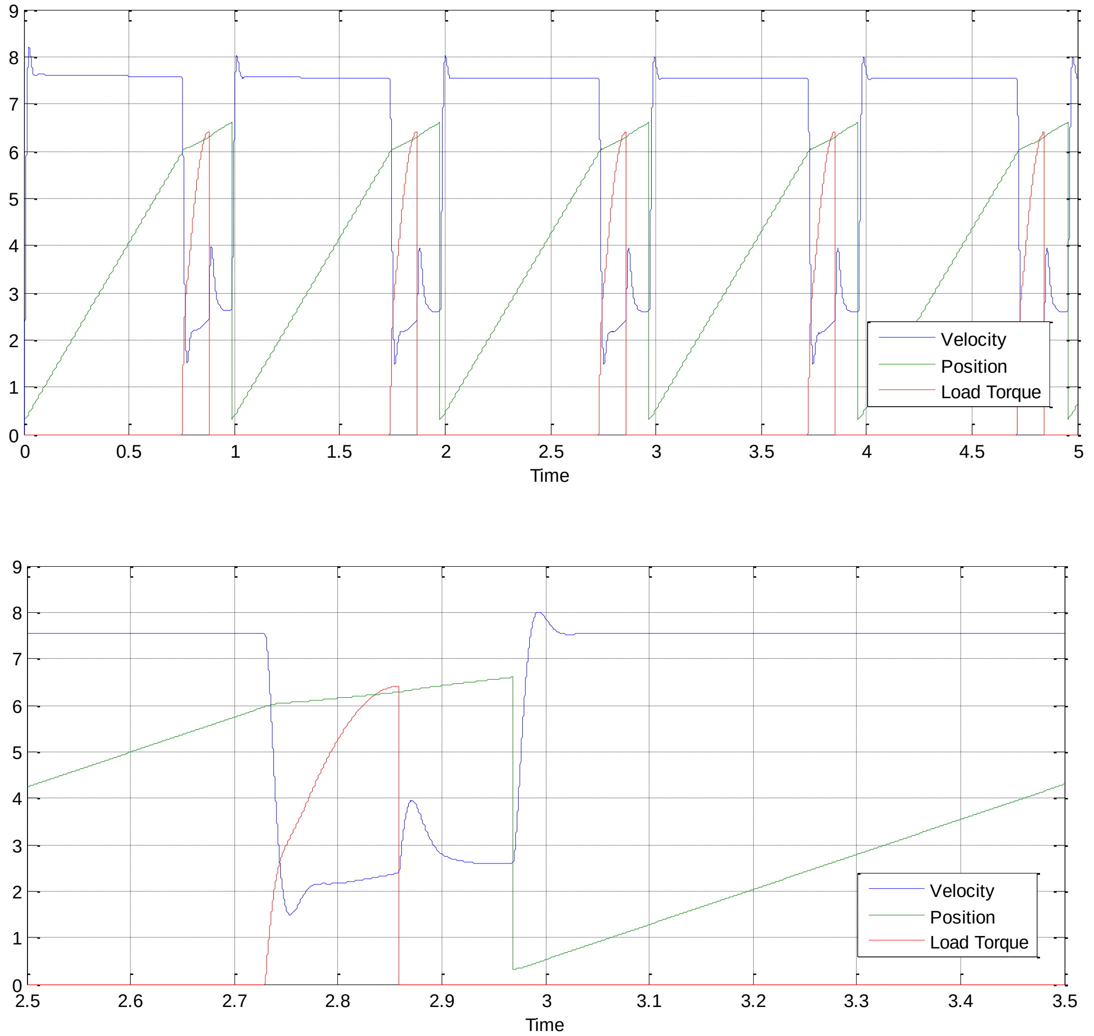

Figure 3.8: Piece length is smaller than the rotary knife circumference

As the piece length is smaller than the rotary knife circumference, the speed in the catch-up zone is faster than the speed in cutting zone. The effect of the load torque (in red) could be observed in Figure 3.8.

The simulated actual cut piece length has an error of 1.07% in this case.

4. CONCLUSIONS AND RECOMMENDATIONS

This study has obtained and analyzed a mathematical model of the cross-cutter system, successfully controlled the rotary knife movements in two different operation zones and proved an alternative to cam profile operation.

4.1 Practical Application of This Study

This study could be applied in the industry to cross-cutter rotary knife systems to obtain more efficient and delicate cutting operations. This improvement could save costs on reduced wastage. The study also could help realize faster systems with high production speeds without compromising security. As the system proves an alternative to cam profile operation, usage of such a control system could cut down operational costs that would be necessary to change cam profiles according to piece length and system speed.

REFERENCES

Hibbeler, Russell C. (2010). Mechanics of materials, Prentice hall; 8 edition (April 1, 2010).

ROCKWELL AUTOMATION. (2005). RSLogix 5000 motion user guide, USA.

Kreyszig, E. (2011). Advanced engineering mathematics, Wiley; 10 edition (August 16).

Ogata, K. (1995). Discrete Time Control Systems, Prentice Hall, 2nd edition, (January 19).

Nise, N.S. (2010). Control Systems Engineering, Wiley; 6 edition (December 14).

APPENDICES

APPENDIX A: MATLAB m.file for system modelling

APPENDIX B: MATLAB Simulink Model for the Cross-Cutter System Simulation

APPENDIX C: MATLAB m.file for Cross-Cutter System Simulation

APPENDIX D: MATLAB m.file for Fourier series expansion function

APPENDIX E: Mathematica code for PID controller design

APPENDIX A

```
syms s
Kp = 255.14368 ;
Ki = 20 ;

A = xlsread('b.xlsx') ;
plot(0.001*A(:,1),A(:,2),0.001*A(:,1),A(:,3))
grid on

Gce = 31011.86 / ( s^2 + 121.1979*s + 31011.86 ) ;
Gpi = ( Kp*s + Ki ) / s ;

G = Gce/(Gpi*(1-Gce));
```

APPENDIX B

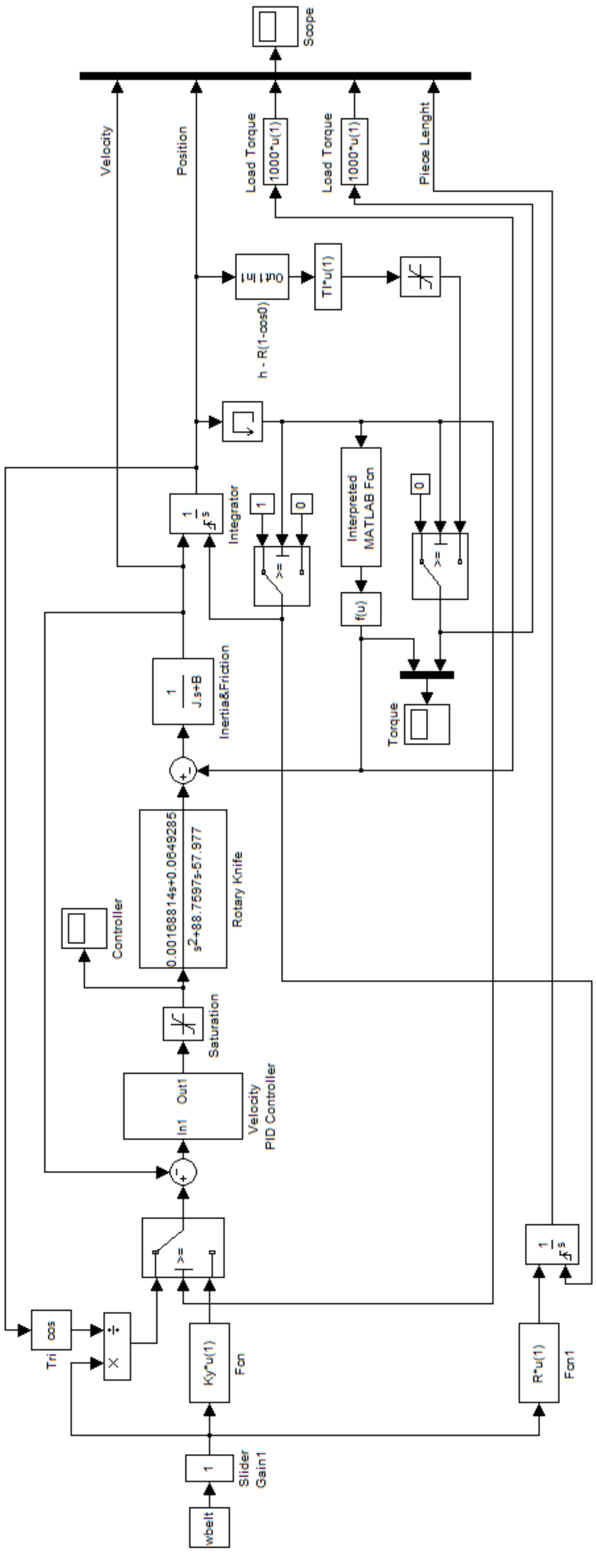

MATLAB Simulink Model for the Cross-Cutter System Simulation

APPENDIX C

```
clear all;
clc

% Motor Parameters %
J = 0.000026 ;
B = 0.001 ;

% Load Parameters %
Vbelt = 50 ;                % (mm/s)
p = 50 ;                    % (mm) parça uzunluğu
R = 20 ;                    % (mm)
h = 1 ;                     % (mm) malzeme kalinligi
d = 2 ;                     % (mm) malzeme genisligi
sigmaUTS = 0.05 ;           % (MPa) celik: 615.4
t=0.001;

% Load Torque calculation %
Tl = 10^-3* ( sigmaUTS*(R^2)*d ) / sqrt( ( 2*R/h )-1 ) ;  % (Nm)

%cut duration angle%
alpha = acos( (R-h)/R );     %(radians)
cutA = 6.28 - alpha ;        %(radians)
% cut completed from point cutA to zero

%Intermeediate variables%
wbelt=Vbelt/R;
L = sqrt(h*(2*R-h));
t_cut = 2*L/Vbelt;
t_catch = (p-2*L)/Vbelt;
Ky = R*(2*pi()-2*alpha)/(p-2*L); %catch-up zone constant => Vk=Vb*Ky
```

APPENDIX D

```
function y = fourier(theta)

A0 = 0.00102845;

y = 0;

for n=3:1:1000

    An = (1/2*pi)*( (0.2432 *( sin(3*n)- sin(3.14*n)) )/n + (1/(n^2-
4))*(-0.143061 *cos(3*n)+0.00163087*cos(3.14*n)-
0.245804*n*sin(3*n)+0.255999*n*sin(3.14*n)));

    Bn = ( 1/ ( 2*n* (n^2-4) )
)*(pi*((0.9728+0.00260359*n^2)*cos(3*n)+(-0.9728-
0.0127987*n^2)*cos(3.14*n)-
0.143061*n*sin(3*n)+0.00163087*n*sin(3.14*n))) ;

    y1=  An*cos(n*pi*theta/(2*pi)) + Bn*sin(n*pi*theta/(2*pi));

    y=y1+y;
end
y = y+A0;
```

APPENDIX E

```
Gce = 31011.86 / (s^2 + 121.1979 * s + 31011.86)

Kp = 255.14368
Ki = 20
Gpi = (Kp * s + Ki) / s

G = Simplify[Gce / (Gpi * (1 - Gce))]
Solve[Denominator[G] == 0, s]

Ts = 0.066008;
Asim = 0.3162;
ξ = -Log[Asim] / √(π^2 + (Log[Asim])^2)
wn = 4 / (ξ Ts)

Gd = wn^2 / (s^2 + 2 ξ wn s + wn^2)

F = (Kdf * s^2 + Kpf * s + Kif) / s

TS = Together[Simplify[F G / (1 + F G)]]

Pds = Denominator[TS]
Pcs = Denominator[Gd]
Pes = a s + b;
S1 = Solve[CoefficientList[Pcs * Pes, s] == CoefficientList[Pds, s]]
```

CURRICULUM VITAE

Name Surname:	Baturalp AKSOY
Place and Date of Birth:	İstanbul, 1987
Address:	Zekeriyaköy Basın Yayın Sitesi, Hanımeli Sokak No: 13 Sarıyer İstanbul
E-Mail:	baturalpaksoy@gmail.com
B.Sc.:	ITU Control Engineering
Professional Experience:	Türk Telekom R&D (2012-present)
	Ford Otosan Product Development (2010-2012)